Available online at www.sciencedirect.com

SCIENCE DIRECT®

Journal of Catalysis 222 (2004) 377–388

JOURNAL OF CATALYSIS

www.elsevier.com/locate/jcat

# $NO_x$ adsorption study over Pt–Ba/alumina catalysts: FT-IR and pulse experiments

Isabella Nova,[a,*] Lidia Castoldi,[a] Luca Lietti,[a] Enrico Tronconi,[a] Pio Forzatti,[a]
Federica Prinetto,[b] and Giovanna Ghiotti[b]

[a] *Dipartimento di Chimica, Materiali e Ingegneria Chimica “Giulio Natta,” Politecnico di Milano, Piazza Leonardo da Vinci 32, 20133 Milan, Italy*
[b] *Dipartimento di Chimica IFM, Università di Torino, Via P. Giuria 7, 10125 Turin, Italy*

Received 4 August 2003; revised 18 November 2003; accepted 19 November 2003

**Abstract**

Adsorption of NO, NO/$O_2$, and $NO_2$ on Pt–Ba–Al–O system is investigated at 350 °C by the transient response method (TRM) and FT-IR spectroscopy. The data suggest that in the presence of oxygen, NO is effectively adsorbed (at a Ba site in proximity of a Pt site) through stepwise oxidation to form at first nitrites that are progressively transformed into nitrates. NO is also oxidized to $NO_2$ over Pt in the presence of oxygen. $NO_2$ is directly adsorbed to form Ba nitrates according to a disproportionation reaction, which occurs with the evolution of NO. The stepwise oxidation route seems to play a major role in $NO_x$ storage from NO/$O_2$ mixtures.

*Keywords:* Lean de$NO_x$; $NO_x$ storage; Lean $NO_x$ trap; Pt–Ba/$\gamma$-$Al_2O_3$; Transient response method; Fourier transform infrared

## 1. Introduction

Engines that operate under lean burn (i.e., oxygen rich) conditions can provide significant fuel economy compared with stoichiometric engines [1]. In the presence of excess oxygen in the exhaust gas, however, $NO_x$ cannot be sufficiently removed by conventional three-way catalysts [2–5]. A promising approach to $NO_x$ removal under lean conditions is based on the $NO_x$ storage-reduction (NSR) concept [6–9]. NSR catalytic systems, also referred to as lean $NO_x$ traps (LNTs), are operated alternatively under lean and rich conditions: $NO_x$ is stored on the catalyst under lean conditions and subsequently converted to nitrogen by unburned hydrocarbons under rich conditions. Typical NSR catalysts consist of a high-surface-area support (e.g., $\gamma$-alumina), a $NO_x$-storage component (an alkaline or earth-alkaline metal oxide), and a noble metal (Pt), for both the oxidation of NO and hydrocarbons and the reduction of stored $NO_x$.

Several articles have recently been published on these catalytic systems, and both the “storage” and “reduction” phases have been investigated [6–27]. However, many aspects of the reaction, and particularly of the $NO_x$ storage mechanism, have not yet been completely clarified. It is generally believed that NO (which predominates in the exhaust gas) is first oxidized to $NO_2$ at platinum and $NO_2$ is then stored on barium. According to this picture, Fridell and co-workers [10] proposed a three-step mechanism in which $NO_2$ is at first loosely adsorbed on BaO as a BaO–$NO_2$ species; this species then decomposes to $BaO_2$ and NO (which is released in the gas phase) and finally Ba peroxide reacts with the gas-phase $NO_2$ to give Ba nitrate:

$$NO_2 + BaO \rightarrow BaO\text{–}NO_2, \tag{1}$$

$$BaO\text{–}NO_2 \rightarrow BaO_2 + NO, \tag{2}$$

$$2NO_2 + BaO_2 \rightarrow Ba(NO_3)_2. \tag{3}$$

The overall stoichiometry of $NO_2$ adsorption ($3NO_2 + BaO \rightarrow Ba(NO_3)_2 + NO$) implies the release of one molecule of NO for the consumption of three molecules of $NO_2$. However, in a previous work the same authors [11] argued that $NO_2$ may also form nitrites on the surface of barium which in turn are oxidized to nitrates by $NO_2$ in a reaction where NO desorbs in the gas phase. In a more recent article, Broqvist et al. [12] suggest that $NO_2$ could be at first adsorbed on $O^{2-}$ sites to form surface nitrates or on $Ba^{2+}$ to form surface nitrites, which evolve to nitrates.

---

[*] Corresponding author.
*E-mail address:* isabella.nova@polimi.it (I. Nova).

0021-9517/$ – see front matter
doi:10.1016/j.jcat.2003.11.013

Hess and Lunsford [14,15], on the basis of in situ Raman studies performed over a BaO/MgO film, proposed the formation of nitro species on $Ba^{2+}$ sites on $NO_2$ admission, which then evolve to nitrite ions with simultaneous formation of amorphous nitrates; on longer $NO_2$ exposure crystalline $Ba(NO_3)_2$ was also formed with evolution of NO. Again, these reactions satisfy the stoichiometry of reactions (1)–(3). In addition, Hess and Lunsford also considered a direct uptake of $NO_2$ to form nitrate species, i.e., with no evolution of NO. Direct $NO_2$ uptake without NO evolution has also been suggested by Cant and Patterson [13].

In addition to $NO_2$, the adsorption of NO has also been investigated. Schmitz et al. [16] identified the species formed when NO and $NO_2$ are exposed at room temperature (RT) on a thin film of barium oxide as nitrite and nitrate species, respectively. More recently, Sedlmair and co-workers [17] studied by in situ IR spectroscopy the surface species and reaction intermediates on a prereduced commercial catalyst during exposure at 50 °C to NO, $NO_2$, and NO/$O_2$. They proposed that at first NO is stored in the form of nitrites on the storage component. $NO_2$ can be formed on the noble metal and then it either adsorbs molecularly and forms nitrates or adsorbs dissociatively and forms nitrites, which are then oxidized by $NO_2$ into surface nitrates. In situ FT-IR experiments were also performed by Huang et al. [18] on $CaO/Al_2O_3$ catalysts. It was found that under lean burn conditions NO and/or $NO_2$ were stored on a prereduced catalyst in the form of nitrate species, with intermediate formation of nitrite and $NO_2$ adsorbed species (ad-species).

The adsorption of NO, $NO_2$, and NO/$O_2$ mixtures at room temperature on Pt–Ba/$Al_2O_3$, Ba/$Al_2O_3$, and Pt/$Al_2O_3$ samples has also been previously investigated in our laboratories by means of FT-IR spectroscopy and temperature-programmed desorption (TPD), and the results are reported elsewhere [19]. The study provided information on the nature, relative amounts, and thermal stability of the stored $NO_x$ species. In this article, an extensive and systematic study has been undertaken to clarify the mechanism of $NO_x$ storage and to better elucidate the role of the different catalyst components and the different gaseous and surface species involved in the process. For this purpose, the adsorption of NO and $NO_2$ in the presence and absence of oxygen was investigated over a Pt–Ba/$\gamma$-$Al_2O_3$ sample, over the corresponding binary samples (Ba/$\gamma$-$Al_2O_3$ and Pt/$\gamma$-$Al_2O_3$), and over the pure support ($\gamma$-$Al_2O_3$). The study was performed under operating conditions representative of real applications, i.e., transient conditions and high temperatures (350 °C). The transient response method (TRM) and FT-IR spectroscopy were used as complementary techniques to analyze both gas phase composition and catalyst surface species formed during the adsorption of $NO_x$. The $NO_x$ adsorbed species were subsequently decomposed by heating the catalyst sample (TPD); accordingly, information on the thermal stability of such adsorbed species is also derived.

## 2. Experimental methods

### 2.1. Catalysts preparation

Pt/$\gamma$-$Al_2O_3$ (1/100 w/w) and Ba/$\gamma$-$Al_2O_3$ (20/100 w/w) samples were prepared by incipient wetness impregnation of a commercial $\gamma$-alumina support (Versal 250 from La Roche Chemicals) calcined at 700 °C. Precursors for Pt and Ba were platinum dinitrodiammine (Strem Chemicals, 5% Pt in ammonium hydroxide) and barium acetate (Strem Chemicals, 98.5%), respectively. After impregnation the powders were dried overnight at 80 °C in air and calcined at 500 °C for 5 h. The ternary Pt–Ba/$\gamma$-$Al_2O_3$ (1/20/100 w/w) catalyst was prepared by incipient wetness impregnation of the calcined Pt/$\gamma$-$Al_2O_3$ sample.

### 2.2. Characterization techniques and reactivity tests

Absorption/transmission IR spectra were obtained with a Perkin–Elmer FT-IR System 2000 spectrophotometer equipped with a Hg–Cd–Te cryodetector, working in the range of wavenumbers 7200–580 $cm^{-1}$ at a resolution of 1 $cm^{-1}$ (number of scans $\sim$ 10). For IR analysis powder samples were compressed in self-supporting disks (10 mg $cm^{-2}$) and placed in a commercial heatable stainless-steel cell (Aabspec), allowing thermal treatments in situ under vacuum or controlled atmosphere and the simultaneous registration of spectra at temperatures up to 600 °C. Before $NO_x$ storage experiments, pellets were activated by heating in dry oxygen at 600 °C, cooled to 350 °C, and evacuated at the same temperature. $NO_x$ storage experiments were performed by admitting NO (Praxair, freshly distilled before use), $NO_2$ (Praxair), or freshly prepared NO/$O_2$ or $NO_2$/$O_2$ 1/4 mixtures at 350 °C. IR spectra were recorded at the same temperature (350 °C) at increasing durations of exposure to the various gases or mixtures. The $NO_x$ storage data reported for Ba/$\gamma$-$Al_2O_3$ and Pt–Ba/$\gamma$-$Al_2O_3$ samples were obtained on samples that were fully conditioned by performing a few previous storage–regeneration cycles consisting of heating in $NO_2$ at 350 °C, evacuation at 600 °C, and heating in dry oxygen at 350 °C, to decompose the $BaCO_3$ phase, according to previous results [19].

The adsorption of $NO_x$ under transient conditions has been investigated by the TRM using a flow microreactor system made of a quartz tube (7 mm i.d.) directly connected to a mass spectrometer (Balzers QMS 200). In a typical experiment 120 mg of catalyst (75–105 µm) was loaded into the reactor and oxidized at 500 °C for 1 h in He + 20% $O_2$. Then a stream of He or He + 3% $O_2$ (200 $cm^3$/min STP) was fed to the reactor and the catalyst temperature was set at 350 °C. After stabilization of the mass spectrometer signals a rectangular step feed of 1000 ppm NO or $NO_2$ was admitted to the reactor, while the reactor outlet concentration was monitored. Finally, when saturation of the catalyst was approached, the NO or $NO_2$ concentration was stepwise decreased back to zero.

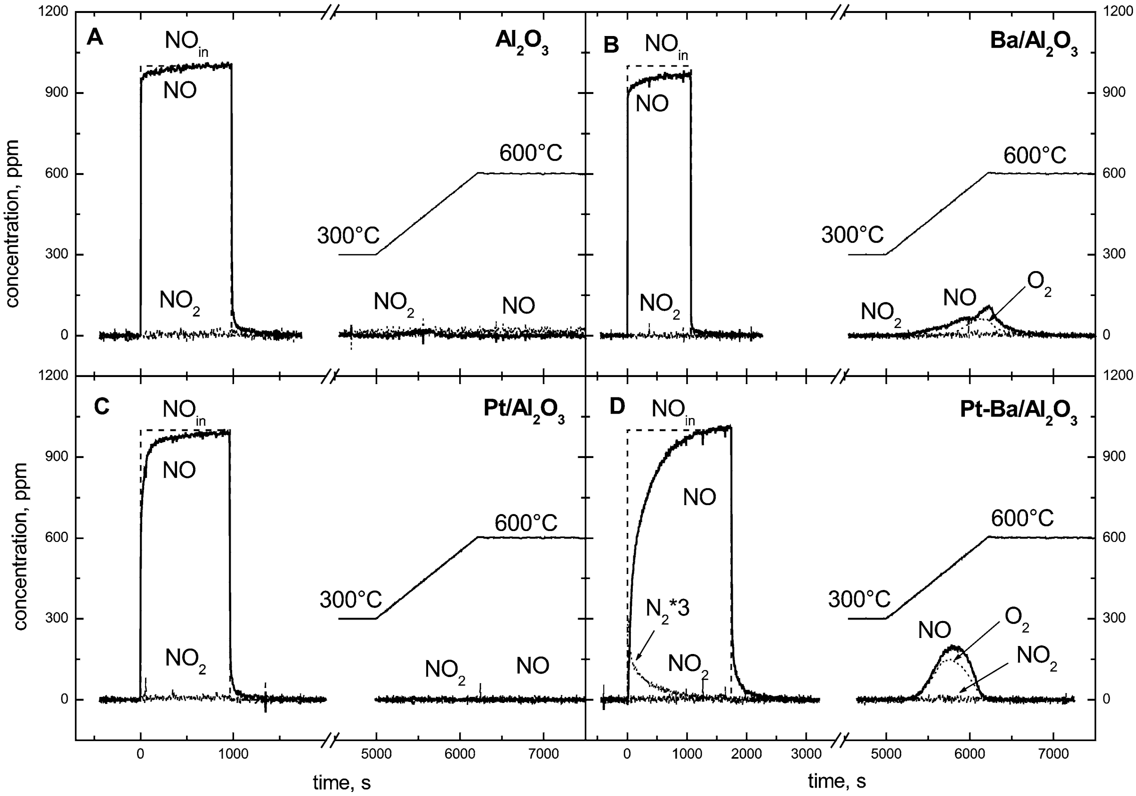

Fig. 1. Results of NO adsorption TRM experiments at 350 °C in He and subsequent TPD in He from 300 to 600 °C over (A) $\gamma$-$Al_2O_3$, (B) Ba/$\gamma$-$Al_2O_3$, (C) Pt/$\gamma$-$Al_2O_3$, and (D) Pt–Ba/$\gamma$-$Al_2O_3$ catalysts in terms of NO, $NO_2$, $O_2$, and $N_2$ outlet concentrations and NO inlet concentration.

The $NO_x$ species adsorbed during TRM experiments were subsequently decomposed by TPD; for this purpose the catalyst was at first cooled to 300 °C in He (flow rate of 200 $cm^3/min$) and then linearly heated to 600 °C at 15 °C/min, followed by a hold of 1 h at 600 °C. The following mass-to-charge ($m/e$) ratios were used to monitor the concentrations of products and reactants: 18 ($H_2O$), 28 ($N_2$), 30 (NO), 32 ($O_2$), 44 ($N_2O$ or $CO_2$), 46 $(NO)_2$. Mass spectrometer data were quantitatively analyzed using the fragmentation patterns and response factors determined experimentally from calibration gases. Further details on the experimental apparatus and procedure can be found elsewhere [19,20].

Data reported in the article were collected on catalyst samples that were conditioned by performing few storage–regeneration cycles until reproducible data could be obtained.

## 3. Results and discussion

### 3.1. Catalyst characterization

The Pt/$\gamma$-$Al_2O_3$ sample is characterized by a large surface area (210 $m^2/g$) and a large pore volume (1.15 $cm^3/g$). Ba-containing samples have lower surface areas (140 and 160 $m^2/g$ for Ba/$\gamma$-$Al_2O_3$ and Pt–Ba/$\gamma$-$Al_2O_3$ catalysts, respectively) and pore volumes (0.80 and 0.82 $cm^3/g$ for Ba/$\gamma$-$Al_2O_3$ and Pt–Ba/$\gamma$-$Al_2O_3$, respectively).

XRD measurements performed over the calcined samples revealed the presence of crystalline $\gamma$-$Al_2O_3$ (JCPDS 10-425) in all the samples, of the orthorhombic form of $BaCO_3$ in Ba/$\gamma$-$Al_2O_3$ catalyst, and of traces of $BaCO_3$ (both monoclinic (JCPDS 78-2057) and orthorhombic (Whiterite, JCPDS 5-378)) in the fresh Pt–Ba/$\gamma$-$Al_2O_3$ catalyst. Quantitative analysis of the XRD spectra indicated that Ba is well dispersed on the surface of the ternary Pt–Ba/$\gamma$-$Al_2O_3$ catalyst. Further details on the characterization data of the samples can be found in previous articles [19,20].

### 3.2. NO adsorption experiments

The results obtained in the case of a rectangular step feed of NO in He at 350 °C and subsequent TPD on the investigated catalyst samples are illustrated in Fig. 1 in terms of NO, $NO_2$, $O_2$ and (if any) $N_2$ concentration with time.

For the $\gamma$-$Al_2O_3$ support (Fig. 1A) and for both the Ba/$\gamma$-$Al_2O_3$ and Pt/$\gamma$-$Al_2O_3$ binary catalysts (Figs. 1B and C), the profiles of the NO outlet concentration closely resemble those of the inlet NO concentrations, indicating that NO does not significantly adsorb on these catalysts (Fig. 2). Formation of other species (e.g., $NO_2$ or $N_2$) has not been observed over the samples investigated. When the NO inlet concentration was reduced back to 0 ppm, a small tail in the NO concentration was observed. Then the TPD run was per-

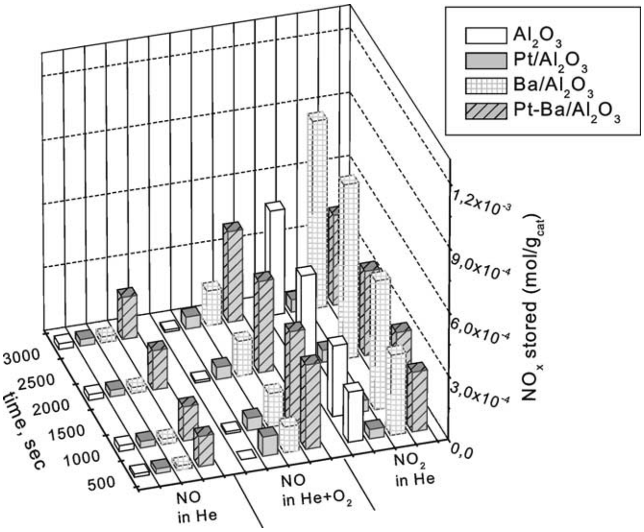

Fig. 2. $NO_x$ adsorbed quantities ($mol/g_{cat}$) during TRM experiments over $\gamma$-$Al_2O_3$, Ba/$\gamma$-$Al_2O_3$, Pt/$\gamma$-$Al_2O_3$, and Pt–Ba/$\gamma$-$Al_2O_3$ catalysts at 350 °C with different feed gases.

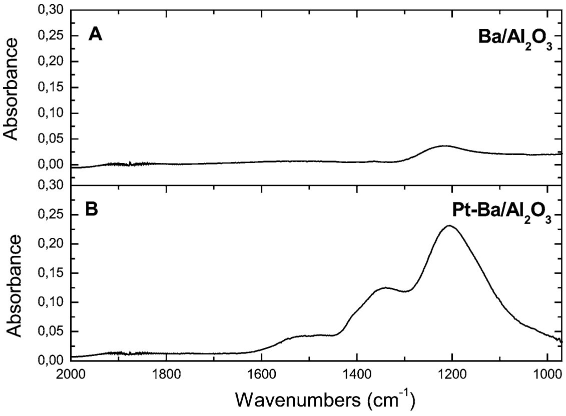

Fig. 3. Results of NO adsorption FT-IR experiments over (A) Ba/$\gamma$-$Al_2O_3$ and (B) Pt–Ba/$\gamma$-$Al_2O_3$ catalysts. Spectra are reported after 5 min of exposure to 5 mbar of NO at 350 °C. Each spectrum is reported as the difference from the spectrum before NO admission.

formed; desorption of NO and $O_2$ (in small amounts) was observed only in the case of Ba/$\gamma$-$Al_2O_3$ sample.

FT-IR analysis confirmed that no surface species were formed on NO admission at 350 °C on the $\gamma$-$Al_2O_3$ support and on the Pt/$\gamma$-$Al_2O_3$ binary catalyst (spectra here not reported); weak bands due to the formation of small amounts of ionic nitrites ($\nu_{asym}$ONO mode near 1220 $cm^{-1}$) were observed in the case of Ba/$\gamma$-$Al_2O_3$ sample (Fig. 3A).

Different results were obtained in the case of the NO pulse experiments performed over Pt–Ba/$\gamma$-$Al_2O_3$ sample (Fig. 1D). On admission of NO to the reactor, the NO outlet concentration exhibits a very short dead time (on the order of seconds) and then slowly increases with time, reaching a steady state value of 1000 ppm. This indicates that $NO_x$ are being stored on the catalyst surface, as also confirmed by the TPD experiment performed at the end of the TRM run.

Also in this case, $NO_2$ was not detected in the gas phase. Notably, at the beginning of the NO pulse, a small $N_2$ evolution was observed, accompanied by the formation of minor amounts of $N_2O$ (not reported in the figure), which is likely an intermediate in the $N_2$ production. The amounts of nitrogen and $N_2O$ produced roughly correspond to the number of accessible Pt sites, as determined by $H_2$ chemisorption measurements reported elsewhere [19]. Formation of $N_2$ and $N_2O$ is likely associated with the reduction of NO on metal Pt centers; since no $N_2$ and $N_2O$ was observed over Pt/$\gamma$-$Al_2O_3$, Ba plays a role in the process. It might be speculated that BaO adsorbs NO, which is then reduced at a neighbor Pt site, or that BaO acts as an “oxygen sink” for Pt, which is kept without adsorbed oxygen. The presence of reduced Pt at the beginning of the pulse can be ascribed to the catalyst regeneration procedure, which involves annealing at 600 °C in He prior to NO adsorption. In fact, when oxygen is present in the gas phase (experiments on NO adsorption in the presence of oxygen, see below) neither $N_2$ formation nor $N_2O$ formation occurs.

FT-IR spectra recorded on NO admission at 350 °C on the Pt–Ba/$\gamma$-$Al_2O_3$ catalyst (Fig. 3B) revealed the presence of ionic nitrites (1220 $cm^{-1}$), formed in larger amounts with respect to Ba/$\gamma$-$Al_2O_3$, in line with the TRM data discussed above. In addition, minor absorptions associated with nitrate species are also evident (broad bands at 1320 and 1410 $cm^{-1}$, due to ionic nitrates, and around 1550 $cm^{-1}$, due to bridging nitrates).

The results reported above suggest that the catalytic surface of Ba-containing samples is characterized by an oxidation function (likely associated with $BaO_2$); accordingly, nitrite species can be formed on interaction of NO with Ba peroxide ions as already proposed by some of us [19]. The major amounts of nitrite species formed in the presence of Pt can be reasonably ascribed to NO decomposition over Pt and subsequent migration of atomic oxygen to the Ba component, with formation of reactive peroxide ions. The presence of a catalyst oxidation function is in line with desorption of oxygen detected during the TPD run. However, during TRM experiments (and the subsequent TPD run) the presence of trace amounts of impurity oxygen in the feed gas cannot be excluded. These oxygen traces may take part in the observed oxidation of NO to surface nitrites. On the other hand, the presence of oxygen in FT-IR measurements can be reasonably excluded due to the NO purification procedure adopted.

### *3.3. $NO_2$ adsorption experiments*

The results obtained in the experiments on adsorption of $NO_2$ in He at 350 °C on the catalysts investigated are illustrated in Fig. 4.

In the case of $\gamma$-$Al_2O_3$ (Fig. 4A), the NO outlet concentration shows a sharp maximum (300 ppm) immediately on $NO_2$ admission and then slowly decreases with time until its concentration becomes nil. Simultaneously, $NO_2$ concentration immediately reaches the value of 300 ppm, and then

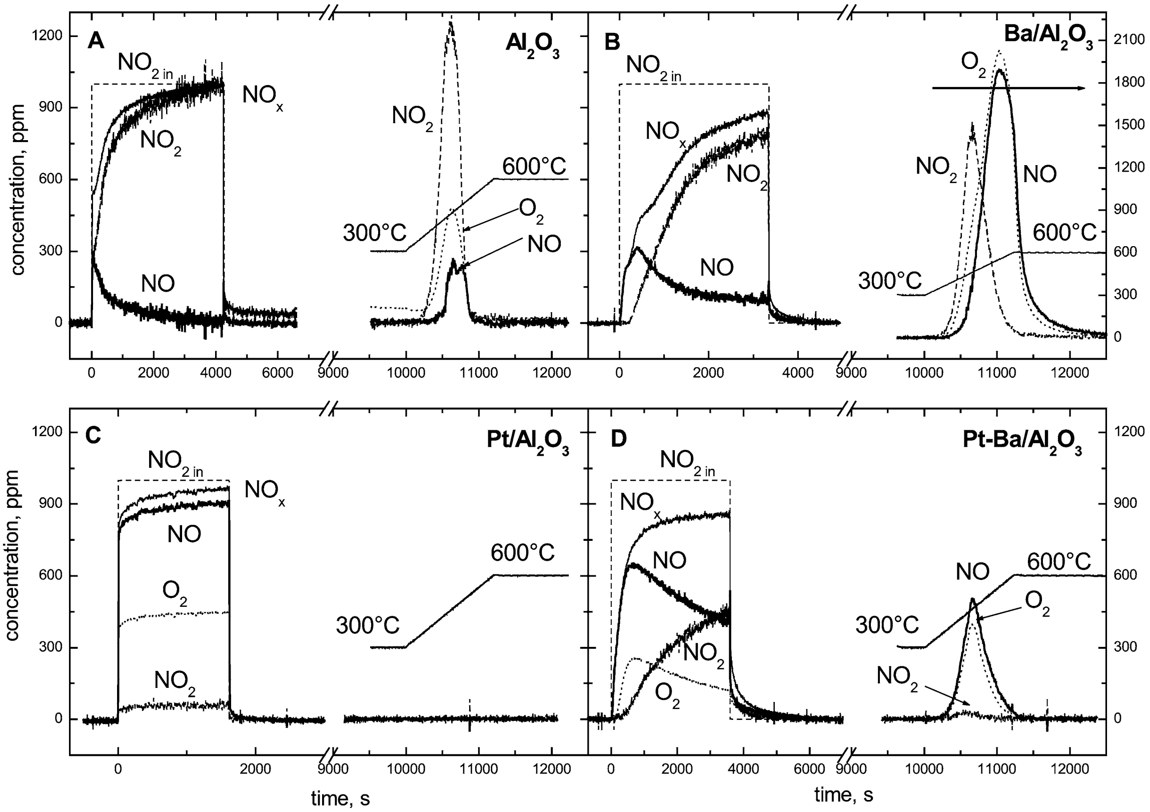

Fig. 4. Results of $NO_2$ adsorption TRM experiments at 350 °C in He and subsequent TPD in He from 300 to 600 °C over (A) $\gamma$-$Al_2O_3$, (B) Ba/$\gamma$-$Al_2O_3$, (C) Pt/$\gamma$-$Al_2O_3$, and (D) Pt–Ba/$\gamma$-$Al_2O_3$ catalysts in terms of NO, $NO_2$, $NO_x$, $O_2$ outlet concentrations and $NO_2$ inlet concentration.

increases more slowly, approaching the inlet $NO_2$ concentration value. Significant amounts of $NO_x$ are stored on the catalyst surface in this case (see Fig. 2); in fact, the subsequent TPD run is characterized by significant desorption of $NO_2$ and $O_2$, with a maximum near 460 °C, and of minor amounts of NO. Hence the data clearly indicate that significant amounts of $NO_x$ can be stored from $NO_2$ on the pure alumina support, and that the storage of $NO_2$ is accompanied by the release of NO. The value of the integral ratio $(= (\int \text{moles NO evolved})/(\int \text{moles NO}_2 \text{ consumed}))$ is shown in Fig. 5A as a function of time. A value near 0.33 is observed immediately after the $NO_2$ step addition and is constant along the whole run: this demonstrates that the $NO_2$ uptake process over alumina produces one NO molecule for every three $NO_2$ molecules consumed, in line with the stoichiometry of reactions (1)–(3).

The FT-IR spectra reported in Fig. 6A indicate that only nitrate species are formed on $NO_2$ adsorption at 350 °C on $\gamma$-$Al_2O_3$ and these are specifically of the bidentate type (1585 $cm^{-1}$, $\nu$NO; 1292, 1255 $cm^{-1}$ $\nu_{\text{asym}}NO_2$; 1030–1000 $cm^{-1}$, $\nu_{\text{sym}}NO_2$). Therefore, it is concluded that in this case $NO_2$ adsorption occurs according to the overall stoichiometry

$$O^{2-} + 3NO_2 \rightarrow 2NO_3{}^{-} + NO\uparrow, \tag{4}$$

which is actually the disproportionation of $NO_2$ to NO and $NO_3{}^{-}$.

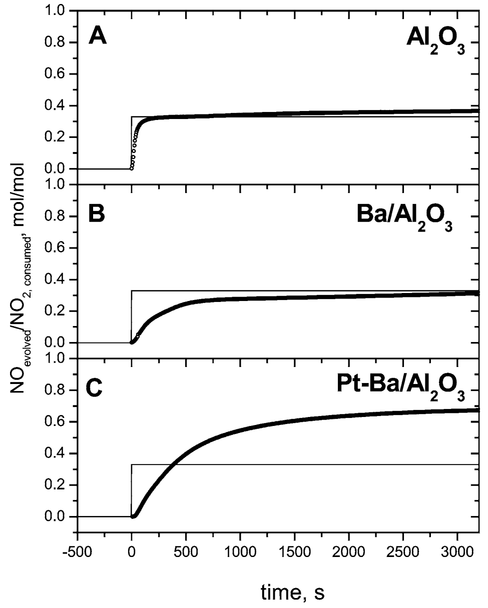

Fig. 5. Ratio of NO evolved to the amounts of $NO_2$ consumed in He over (A) $\gamma$-$Al_2O_3$, (B) Ba/$\gamma$-$Al_2O_3$, and (C) Pt–Ba/$\gamma$-$Al_2O_3$ catalysts.

Like the bare alumina support, also in the case of Ba/$\gamma$-$Al_2O_3$ sample, $NO_2$ storage is accompanied by the evolution of NO (Fig. 4B), but the NO and $NO_2$ concentration profiles present in this case different dynamics. In fact, the NO outlet concentration shows a maximum of 300 ppm 400 s

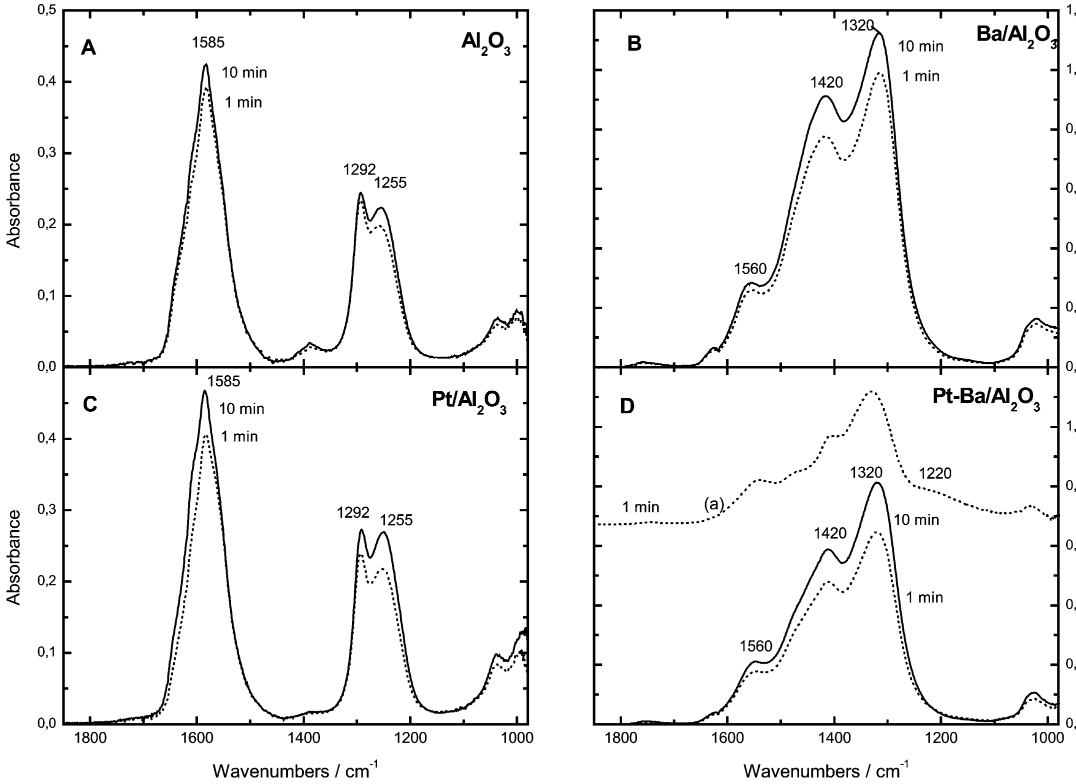

Fig. 6. Results of $NO_2$ adsorption FT-IR experiments over (A) $\gamma$-$Al_2O_3$, (B) Ba/$\gamma$-$Al_2O_3$, (C) Pt/$\gamma$-$Al_2O_3$, and (D) Pt–Ba/$\gamma$-$Al_2O_3$ catalysts. Spectra are reported after 1 and 10 min of exposure to 5 mbar of $NO_2$ at 350 °C. Trace (a): spectrum recorded after 1 min of exposure to $NO_2$ on a pre-reduced Pt-Ba/$Al_2O_3$ system. Each spectrum is reported as the difference from the spectrum before $NO_2$ admission.

after $NO_2$ admission, whereas the $NO_2$ outlet concentration trace exhibits a dead time of 200 s and then slowly increases to reach a final value of 700 ppm. Large amounts of $NO_x$ are stored on the catalyst surface in this case (see Fig. 2); notably, at the end of the adsorption pulse, the outlet $NO_x$ concentration has not yet reached the inlet value, indicating that $NO_x$ are still being stored on the catalyst surface. During the subsequent TPD experiment, $NO_2$ desorption was observed starting from 370 °C with a maximum at 470 °C, while NO and oxygen showed peaks at higher temperature (with maxima close to 560 °C).

FT-IR data reported in Fig. 6B show that only nitrate species were formed on $NO_2$ adsorption, and were mainly of the ionic type (bands at 1320, 1420–40 $cm^{-1}$, $\nu_{asym}NO_3$ split for the partial removal of the degeneracy; 1035–20 $cm^{-1}$, $\nu_{sym}NO_3$) and, in minor amounts, bidentate (1560 $cm^{-1}$, $\nu_{NO}$; $\nu_{asym}NO_2$ mode expected around 1300 $cm^{-1}$ obscured by the modes of ionic nitrates). The nitrate species adsorbed over Ba/$\gamma$-$Al_2O_3$ exhibited higher thermal stability than those on the bare alumina support, as indicated out by TPD, due to the higher basicity of BaO as compared with $Al_2O_3$. Notably, the adsorbed nitrates are related to the Ba component as the surface of the alumina support is almost completely covered by Ba, as indicated out by FT-IR data previously reported [19].

Over the supported Ba samples the integral ratio (Fig. 5B) is initially lower than the stoichiometric value (0.33). This indicates that $NO_2$ uptake at the beginning of the pulse does not obey the overall stoichiometry of reaction (4); however, the stoichiometric value is roughly approached at the end of the pulse, after 3300 s. Hence the stoichiometry of the disproportionation reaction (4) accounts almost quantitatively for $NO_x$ storage from $NO_2$ over Ba/$\gamma$-$Al_2O_3$.

A deviation of the NO evolved/$NO_2$ consumed ratio with respect to the stoichiometric value 0.33 has already been pointed out by Cant and Patterson [13] over both $\gamma$-$Al_2O_3$ and Ba/$\gamma$-$Al_2O_3$ at the beginning of $NO_x$ storage from $NO_2$. These authors considered an initial parallel $NO_2$ uptake without evolution of NO, leading to the formation of coordinately bonded surface species, e.g., nitro or nitrito group. Since FT-IR spectra (Fig. 6B) did not show any difference in the nature of the species detected at the beginning of the pulse, it can be argued that $NO_2$ is directly stored in the form of nitrates without NO release, which implies the participation of a catalyst oxidation function in the storage process. The existence of $O_2^{2-}$ ions prior to $NO_2$ admission can be reasonably accounted for by the formation of Ba peroxide phases or defect-rich BaO during the sample activation-conditioning pretreatments (see Experimental methods). Indeed, there are indications in literature [19,21] for the formation of peroxide ions in or on defective BaO during the decomposition of $Ba(NO_3)_2$. Moreover, crystalline $BaO_2$ was detected by Raman spectroscopy when the decomposition was carried out in the presence of oxygen [21].

However, the observation that a value of 0.33 of the Integral Ratio is roughly approached at the end of the $NO_2$ adsorption step suggests the minor role (if any) of routes other than the $NO_2$ disproportionation pathway (reaction (4)); i.e., the $NO_2$ disproportionation reaction is able to account almost completely for the $NO_2$ uptake at saturation. In fact, the initial departure of the value of the integral ratio from the expected value of 0.33 can be also accounted for by the mechanism suggested by Fridell et al. [10–12] and Hess and Lunsford [14,15]. Indeed, one can speculate that the first step in the disproportionation reaction (which does not lead to NO evolution, reaction (1)) is fast, and that this step is followed by a slower reaction of the adsorbed intermediate with NO evolution (reactions (2)+(3)). In fact, this hypothesis would lead to an initial departure of the integral ratio with respect to the stoichiometric ratio. It is therefore concluded that: (i) Over both Ba/$\gamma$-$Al_2O_3$ and the bare $\gamma$-$Al_2O_3$ support, the $NO_2$ disproportionation reaction almost quantitatively accounts for all of the nitrates stored up to catalyst saturation. (ii) Over Ba/$\gamma$-$Al_2O_3$ the kinetics of the overall process is characterized by two major steps: in the first step an intermediate species is formed, which then evolves to $Ba(NO_3)_2$ ad-species with evolution of NO. In the case of the bare $\gamma$-$Al_2O_3$ support the rates of the two steps of $NO_2$ disproportionation are high and comparable and thus kinetically undistinguishable; however, it is not possible to exclude that the reaction may also proceed according to a different mechanism if compared with Ba/$\gamma$-$Al_2O_3$.

The results obtained on $NO_2$ admission over Pt/$\gamma$-$Al_2O_3$ catalyst are shown in Fig. 4C. In this case, NO, $O_2$, and $NO_2$ are immediately observed at the reactor outlet. Their concentrations rapidly increase with time, reaching steady-state values of 100 ppm for $NO_2$, 450 ppm for $O_2$, and 900 ppm for NO. These values well correspond to the thermodynamic equilibrium for the reaction,

$$NO_2 \leftrightarrow NO + \tfrac{1}{2}O_2, \tag{5}$$

which accordingly is established over this catalyst sample (at the investigated temperature $K_p = 0.19$ vs $K_{eq} = 0.13$ at 350 °C, where $K_p$ and $K_{eq}$ are the experimental partial pressure constant and the equilibrium constant of reaction (5), respectively). It is worth noting that Pt/$\gamma$-$Al_2O_3$ sample showed negligible $NO_x$ storage capability on $NO_2$ exposure, since on Pt sites $NO_2$ immediately decomposes to NO and oxygen. In fact, alumina is not able to significantly adsorb NO in the presence of oxygen, as discussed below.

Finally, $NO_2$ adsorption experiments have been performed over the Pt–Ba/$\gamma$-$Al_2O_3$ sample (Fig. 4D). The formation of NO is observed, showing a maximum of about 600 ppm, followed by a prolonged tail. On the other hand, $NO_2$ concentration exhibits a dead time (280 s) followed by a slow increase. $O_2$ formation has also been observed in this case; its concentration has a dead time of about 200 s and then increases with time, reaching a maximum close to 250 ppm at 650 s. At the end of the storage run the thermodynamic equilibrium $NO_2$/NO is not approached.

The results of $NO_2$ adsorption over Pt–Ba/$Al_2O_3$ can be rationalized by considering three distinct functionalities: (i) Initially ($t = 0$–50 s) $NO_2$ adsorption occurs through the mechanism already proposed for Ba/$\gamma$-$Al_2O_3$ which results in the formation of nitrate species without NO release or considering a rapid first step of the disproportionation reaction (reaction (1)) and a slower rate for the subsequent steps responsible for the evolution of NO (reactions (2) and (3)). (ii) After 50 s the slower elementary steps of the disproportionation route proceed, leading to formation of surface Ba nitrates $Ba(NO_3)_2$ with NO evolution. (iii) While $NO_2$ storage on Ba proceeds further, the Pt-catalyzed $NO_2$ decomposition to NO and $O_2$ becomes appreciable, as indicated out by the evolution of $O_2$ observed at $t > 200$ s. In agreement with this picture, the value of the time-averaged molar NO evolved/$NO_2$ consumed ratio for the Pt–Ba/$\gamma$-$Al_2O_3$ catalyst (Fig. 5C) is lower than 0.33 in the initial period, while it is characterized by higher values for exposure times greater than 400 s after $NO_2$ admission.

In addition, from the data reported above it is also apparent that Pt-catalyzed $NO_2$ decomposition to NO and oxygen is less favored on the ternary system than on the Pt/$\gamma$-$Al_2O_3$ binary sample. An inhibition effect due to the presence of Ba on the reactivity of Pt in the oxidation of NO to $NO_2$ has been already observed by some of us [28] and ascribed to the strong electronic interaction between the alkaline-earth oxide and the noble metal, evidenced by IR data. However, the fact that Pt seems not to be active initially ($t < 200$ s) in $NO_2$ decomposition to NO and $O_2$ could be explained by considering that Ba sites strongly compete in the adsorption of $NO_2$ molecules. Indeed, on one hand, $NO_2$ adsorption on the Ba component occurs immediately as seen in case of Ba/$\gamma$-$Al_2O_3$ catalyst; on the other hand, the number of Ba atoms relative to Pt is very high (Ba/Pt atomic ratio $= 29/1$), so that the interaction of $NO_2$ with Ba oxygen sites is statistically favored. It must also be noted that, after this initial period, the reactivity of Pt over Pt–Ba/$\gamma$-$Al_2O_3$ sample toward $NO_2$ decomposition reaches a maximum and then decreases with time on stream. This clearly indicates that Pt activity decreases as the catalyst becomes saturated: it could be argued that the accumulation of nitrates on Ba sites, which are in proximity to Pt, as previously demonstrated [19], inhibits the reactivity of Pt sites toward $NO_2$ decomposition. A similar effect has also observed by Olsson et al. [11,27], who suggested that $NO_2$ can oxidize Pt particles into inactive Pt oxide, that Pt particles are covered by Ba nitrates, or that some pores could be blocked by Ba nitrates. Since our binary Pt/$\gamma$-$Al_2O_3$ sample did not show any deactivation effect, it could be argued that Pt oxidation to PtO by $NO_2$ is of minor importance in the deactivation process.

Finally, the TPD run performed to regenerate the ternary system revealed the evolution of NO and oxygen at lower temperatures with respect to Ba/$\gamma$-$Al_2O_3$ (470 °C vs 560 °C), while $NO_2$ evolution was not observed. These features can

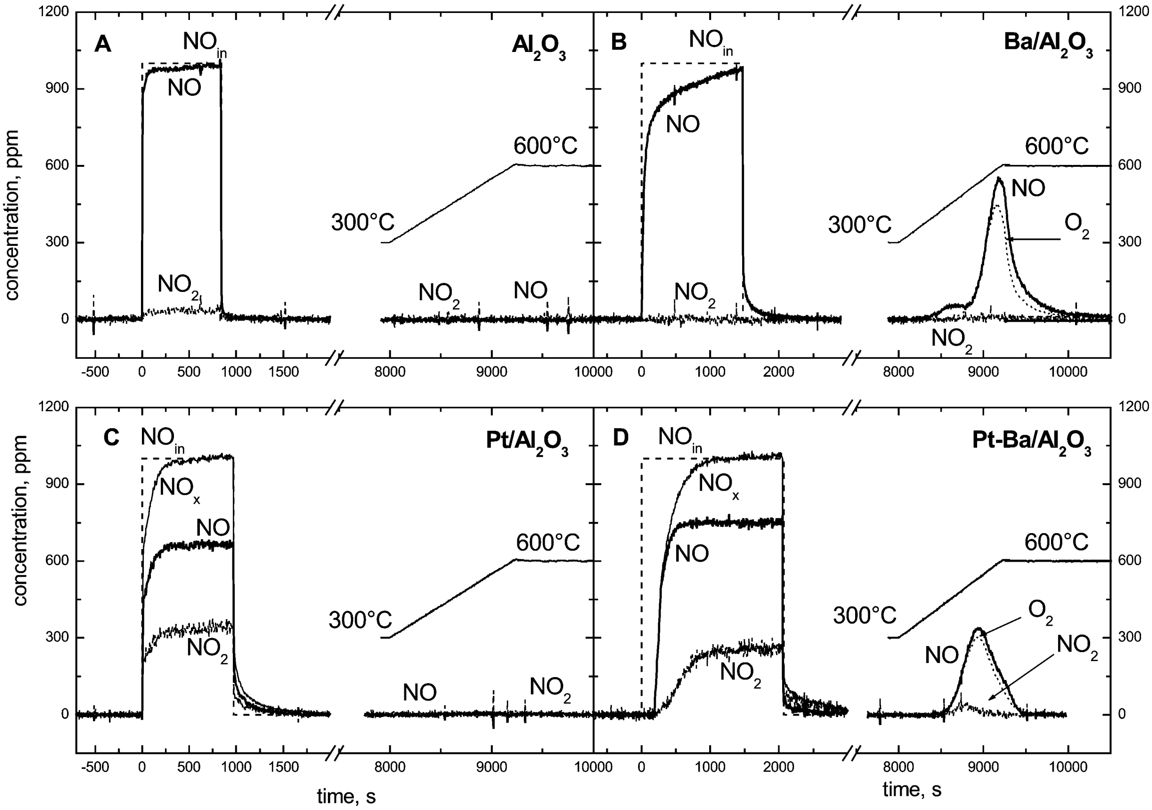

Fig. 7. Results of NO adsorption TRM experiments at 350 °C in He + $O_2$ and subsequent TPD in He from 300 to 600 °C over (A) $\gamma$-$Al_2O_3$, (B) Ba/$\gamma$-$Al_2O_3$, (C) Pt/$\gamma$-$Al_2O_3$, and (D) Pt–Ba/$\gamma$-$Al_2O_3$ catalysts in terms of NO, $NO_2$, $NO_x$, and $O_2$ outlet concentrations and NO inlet concentration.

be ascribed to the presence of Pt, which favors the decomposition of both nitrate species and of $NO_2$ [19].

FT-IR spectra collected over Pt/$\gamma$-$Al_2O_3$ and Pt–Ba/$\gamma$-$Al_2O_3$ catalysts (Figs. 6B and D, respectively) point out that mainly nitrate species were formed on $NO_2$ adsorption. Specifically, on Pt/$\gamma$-$Al_2O_3$ small amounts of bidentate nitrate species were formed, while on Pt–Ba/$\gamma$-$Al_2O_3$, nitrates, mainly of the ionic type (with minor amounts of bidentate species), were formed to a great extent. In both cases the presence of Pt induced a decrease (around 20–30%) in the integrated intensity of the nitrate bands with respect to the parent Pt-free materials, in line with the fact that Pt is active in $NO_2$ decomposition. Notably, if $NO_2$ adsorption is carried out on a prereduced Pt–Ba/$\gamma$-$Al_2O_3$ catalyst, small amounts of nitrites are detected along with nitrates after 1 min of exposure (trace a in Fig. 6D). Nitrites are completely transformed into nitrates after 2–3 min of exposure (not shown in the figure). This datum is in agreement with what is reported in the literature, since many authors [15–18] have pointed out the formation of nitrites on interaction of $NO_2$ with Ba-based catalysts. Our data indicate that nitrate species are the only species formed starting from $NO_2$ gaseous mixture when the catalyst surface is oxidized; on the contrary, if the catalyst is reduced to a certain extent, $NO_2$ can interact with the surface giving rise to minor amounts of nitrites, besides nitrates.

Finally, it is worth noting that the amounts of $NO_x$ stored over $\gamma$-$Al_2O_3$ and Pt/$\gamma$-$Al_2O_3$ are quite different ($4.9 \times 10^{-4}$ moles vs $5.8 \times 10^{-5}$ moles per $g_{cat}$ after 3000 s, Fig. 2), despite the fact that in both cases the $Al_2O_3$ support is involved in storage. This difference can be explained by considering that Pt/$\gamma$-$Al_2O_3$ sample is active in the decomposition of $NO_2$, so that the actual $NO_2$ concentration in this case is very low. On the other hand, FT-IR spectra recorded in the cases of $\gamma$-$Al_2O_3$ and Pt/$\gamma$-$Al_2O_3$ reveal a different picture, in that the amounts of adsorbed $NO_x$ are similar in the two cases. A possible explanation for this apparent discrepancy may be related to the different operating conditions, i.e., static conditions in FT-IR measurements versus flow conditions in TRM experiments. In fact, it can be argued that under the static conditions of the FT-IR measurements the $NO_2$ decomposition reaction does not reach thermodynamic equilibrium and $NO_2$ is available for adsorption. Pt-catalyzed $NO_2$ decomposition to NO may also be invoked to explain the smaller amounts of $NO_x$, that have been stored on Pt–Ba/$\gamma$-$Al_2O_3$ with respect to Ba/$\gamma$-$Al_2O_3$.

### 3.4. NO + $O_2$ adsorption experiments

In the presence of oxygen NO is not significantly adsorbed on the bare $\gamma$-$Al_2O_3$ support (Fig. 7A), similarly to what was already observed in the absence of oxygen (see Fig. 1A). In line with these results, FT-IR data obtained on

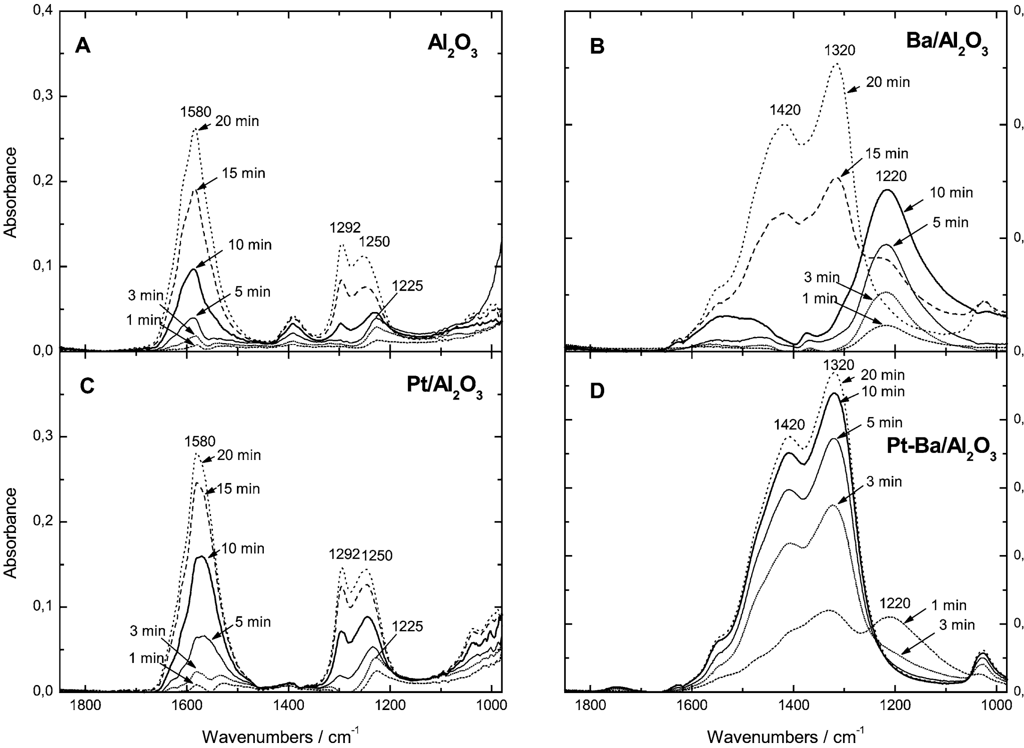

Fig. 8. Results of NO/$O_2$ adsorption FT-IR experiments over (A) $\gamma$-$Al_2O_3$, (B) Ba/$\gamma$-$Al_2O_3$, (C) Pt/$\gamma$-$Al_2O_3$, and (D) Pt–Ba/$\gamma$-$Al_2O_3$ catalysts. Spectra are reported after 1, 3, 5, 10, 15, and 20 min of exposure to NO/$O_2$ mixtures (1:4, $p_{NO} = 5$ mbar) at 350 °C. Each spectrum is reported as the difference from the spectrum before NO/$O_2$ admission.

admission of NO/$O_2$ mixtures at 350 °C on the $\gamma$-$Al_2O_3$ support (Fig. 8A) show that at short exposure times (up to 5 min) only very small amounts of surface nitrites are formed (weak band at 1225 cm$^{-1}$), which are then slowly oxidized to bidentate nitrate species. These species are similar to those formed on $NO_2$ admission, but their amounts are lower (compare Figs. 8A and 6A). The amounts of $NO_x$ stored over the $\gamma$-$Al_2O_3$ support during the FT-IR experiment with NO/$O_2$ are higher than those expected on the basis of TRM results; as discussed before, this apparent disagreement can be explained by considering that the effective contact time between NO and $O_2$ and the catalyst surface during the transient experiments is markedly shorter than under the static conditions of the IR cell.

In the case of Ba/$\gamma$-$Al_2O_3$ sample (Fig. 7B) small quantities of $NO_x$ species are adsorbed on the catalyst surface, as also confirmed by TPD. FT-IR spectra recorded in this case at different exposure times are displayed in Fig. 8B. Ionic nitrites (1220 cm$^{-1}$) were progressively formed on increasing exposure time up to 10 min, along with small amounts of bridging nitrates. At longer exposure times, the band due to nitrite species decreased in intensity and completely disappeared after 20 min. In parallel, bands characteristic of ionic nitrate (1420, 1320, 1030 cm$^{-1}$) and in minor amounts of bidentate nitrates develop, so that after 20 min of exposure only nitrates are evident in the spectra. At these long exposure times the spectra resemble those obtained on $NO_2$ admission (see Fig. 8B vs Fig. 6B); however, the amounts of nitrates formed on adsorption of NO/$O_2$ were markedly lower (about 50%). The possible routes leading to the formation of nitrites and nitrates on a metal oxide surface on admission of NO and oxygen were discussed in a previous article [19]. These reactions involve oxidation of NO by $O_2$, likely activated by the catalyst surface, and interaction with partially uncoordinated surface oxygen anions.

On the Pt/$\gamma$-$Al_2O_3$ catalyst, NO adsorption in the presence of $O_2$ results in the production of large amounts of $NO_2$ in the gas phase: this clearly indicates that NO is rapidly oxidized by $O_2$ to $NO_2$. In fact, the NO, $NO_2$ and $O_2$ concentrations approach those of chemical equilibrium with respect to reverse reaction (5). No dead time is observed on NO addition to the reactor, indicating negligible adsorption of this species over Pt/$\gamma$-$Al_2O_3$ sample. Minor amounts of $NO_x$ are stored during NO adsorption phase (as indicated by the area between the inlet and outlet $NO_x$ concentration traces); however, these amounts are desorbed when the NO concentration is decreased back to zero. This indicates that weakly adsorbed species are formed on NO adsorption in the presence of $O_2$. The negligible $NO_x$ storage is also confirmed by TPD experiments performed at the end of the NO pulse.

FT-IR spectra recorded on admission of NO/$O_2$ mixtures at 350 °C on Pt/$\gamma$-$Al_2O_3$ sample (Fig. 8C) are similar to those observed in the case of the pure alumina support (Fig. 8A): very small amounts of surface nitrites are formed at short exposure times (up to 5 min) and are then slowly oxidized to nitrate species. Note that with respect to pure alumina, the presence of Pt slightly increased the rate of nitrate formation.

Finally, NO adsorption in the presence of oxygen was carried out over Pt–Ba/$\gamma$-$Al_2O_3$ catalyst (Fig. 7D). The NO outlet concentration shows a dead time of 180 s and then increases slowly with time, up to a steady-state value of about 750 ppm. Likewise, $NO_2$ concentration shows a slightly higher breakthrough time with respect to NO ($\approx$ 200 s vs 180 s) and a much slower approach to its steady state value, close to 250 ppm. It is worth noting that this is the only case among our data in which the $NO_x$ outlet concentrations are characterized by a dead time; accordingly this seems to be a peculiar feature of the ternary system and of the presence of gaseous oxygen. Large amounts of $NO_x$ have been stored on the catalyst surface in this case, as also confirmed by TPD experiments performed at the end of the NO pulse (see Fig. 7D).

FT-IR spectra on adsorption of NO/$O_2$ mixtures at 350 °C on Pt–Ba/$\gamma$-$Al_2O_3$ catalyst at different exposure times are displayed in Fig. 8D. Nitrites and nitrates are also observed in this case, but significant differences are noted with respect to the binary Ba catalyst. Indeed, the nitrite band reaches its maximum intensity after 1 min of exposure to the NO/$O_2$ mixture; at this exposure time nitrate species are already detected in large amounts. After 3–5 min of exposure only ionic nitrate species (and in minor amounts, bidentate species) are evident on the catalyst surface. After 5–10 min the nitrate bands have reached their maximum intensity, whereas the increase in the intensity of nitrate bands on Ba/$\gamma$-$Al_2O_3$ sample proceeds up to 20 min.

So, on one hand, NO/$O_2$ storage in the form of nitrate species can occur through the intermediacy of nitrite species. Notably, the rates of both nitrite formation and their oxidation to nitrates are higher on Pt–Ba/$\gamma$-$Al_2O_3$ than on Ba/$\gamma$-$Al_2O_3$, pointing to a catalytic role for Pt. This can possibly be accounted for by $O_2$ dissociation over Pt and subsequent migration of atomic oxygen on the Ba phase. On the other hand, oxidation of NO (on Pt sites) to $NO_2$ by $O_2$ can occur. The first route has been also confirmed by DRIFT data recorded in a flow reaction chamber on the same Pt–Ba/$\gamma$-$Al_2O_3$ sample with NO/$O_2$ mixtures [25], which confirm the initial formation of nitrite species and their progressive transformation into nitrates. Notably, during DRIFT experiments the time corresponding to the maximum in nitrite band intensity corresponds to the NO breakthrough observed by TRM, clearly indicating that up to breakthrough the storage process involves mainly the formation of adsorbed nitrites.

It is therefore concluded that: (i) over both Ba/$\gamma$-$Al_2O_3$ and Pt–Ba/$\gamma$-$Al_2O_3$ NO in the presence of oxygen is initially stored primarily in the form of nitrites; (ii) nitrites are progressively oxidized to nitrates; (iii) Pt promotes the formation of nitrites and their oxidation to nitrates; (iv) the dead time observed for $NO_x$ breakthrough in the case of Pt–Ba/$\gamma$-$Al_2O_3$ sample is related to the rapid formation of nitrite species; (v) Pt also promotes NO oxidation to $NO_2$, and, thus, the first mechanism operates simultaneously with the $NO_2$ storage mechanism already proposed in the case of $NO_2$ adsorption experiments; (vi) at catalyst saturation, nitrates are the most abundant adsorbed species.

### 3.5. *Reaction pathway for $NO_x$ adsorption over supported Pt–Ba catalysts*

The data presented and discussed so far point out the most relevant peculiarities of $NO_x$ storage over Ba-containing NSR catalysts. In particular:

1. Large amounts of $NO_x$ are stored in the form of nitrates on $NO_2$ adsorption over Ba-containing catalysts. The formation of nitrate species occurs via a disproportionation reaction, which involves the evolution of one NO molecule for three $NO_2$ molecules involved in the reaction. The disproportionation reaction is also clearly monitored in the case of the bare $\gamma$-$Al_2O_3$ support, whereas in the presence of Pt, primarily $NO_2$ decomposition to NO and $O_2$ is observed.
2. Negligible amounts of NO are adsorbed on Ba/$\gamma$-$Al_2O_3$ and Pt–Ba/$\gamma$-$Al_2O_3$ catalysts in the form of nitrite adspecies that are likely formed at $BaO_2$ sites.
3. The presence of $O_2$ enhances the adsorption of NO on Ba/$\gamma$-$Al_2O_3$ and particularly on Pt–Ba/$\gamma$-$Al_2O_3$. Opposite to $NO_2$ adsorption, the $NO_x$ storage in this case occurs via formation of both nitrite and nitrate ad-species; nitrites are initially the most abundant species, and they are then progressively transformed into nitrates so that at saturation mainly nitrate species are present on the catalyst surface.
4. In both Ba/$\gamma$-$Al_2O_3$ and Pt–Ba/$\gamma$-$Al_2O_3$ samples, no $NO_x$ adsorbed species have been observed over the support due to the extensive Ba coverage.

Notably, the data show that the formation of nitrites is peculiar to the interaction with NO/$O_2$ mixtures since $NO_2$ adsorption leads to the formation of nitrates only, even at the very beginning of the adsorption process. Hence the adsorption of $NO_x$ from NO/$O_2$ follows a different pathway with respect to the $NO_2$ disproportionation route discussed above, although at saturation in both cases nitrate adsorbed species predominate on the catalyst surface. In particular, in the case of NO/$O_2$, it is suggested that gaseous $O_2$ is activated by Pt sites and transferred to neighbor Ba sites. This would favor a stepwise oxidative adsorption of NO in the form of nitrite-like ad-species on the Ba sites. Notably, opposite to the disproportionation route involving $NO_2$ and leading to the formation of nitrates and NO, the formation of nitrites from NO/$O_2$ mixtures does not involve any NO evolution on storage. Accordingly, a cooperative effect between Pt–Ba neighboring couples appears to be relevant for this route. In fact, several data converge to support the existence of Pt–Ba proximity over the ternary Pt–Ba/$\gamma$-$Al_2O_3$ sample. For instance, CO chemisorption measurements carried out in a previous study [19] clearly indicated a strong

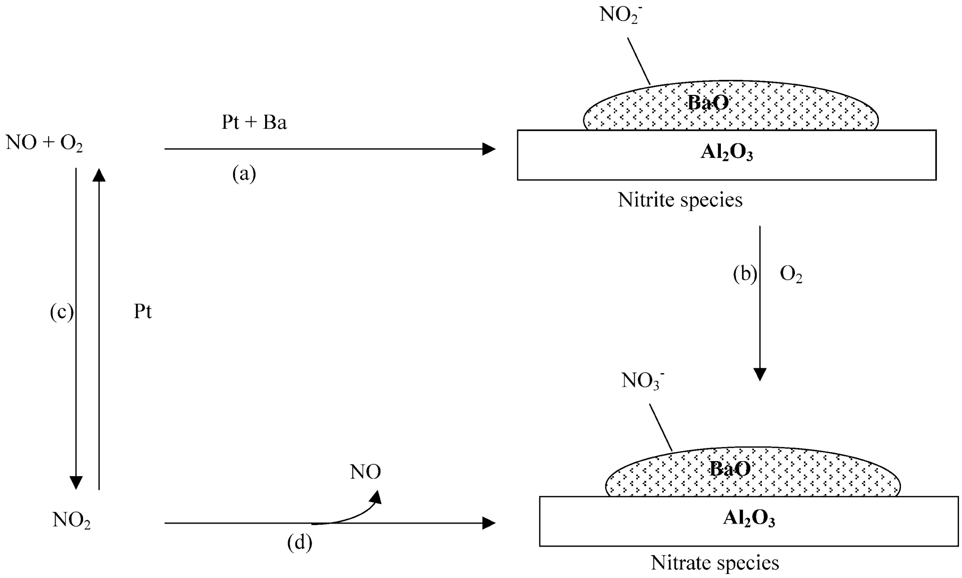

Scheme 1. Reaction pathway for $NO_x$ adsorption over supported Pt–Ba catalysts.

interaction between Pt and the strongly basic oxygen anions of the Ba phase, thus suggesting that the exposed Pt sites and the Ba component are in close proximity. Also, the observation that the thermal stability of adsorbed Ba nitrate species is decreased in the presence of Pt is in line with the existence of a Pt–Ba interaction.

On this basis, the reaction pathway depicted in Scheme 1 is suggested for $NO_x$ adsorption over supported Pt–Ba catalysts. According to the proposed scheme, in the presence of $NO/O_2$ mixtures (the actual gases in the exhausts), $NO_x$ are stored on Ba neighboring Pt sites in the form of nitrite ad-species (route a). Nitrite ad-species are then progressively oxidized to nitrates, which prevail at saturation (route b). Our data point out that routes (a) + (b) (hereafter called "nitrite route") occur on the binary Ba/$\gamma$-$Al_2O_3$ catalyst as well, although to a negligible extent if compared with Pt–Ba/$\gamma$-$Al_2O_3$. Hence the presence of neighboring Pt and Ba sites is important for this route, as previously discussed. Accordingly, Pt plays a role in both the formation of nitrites and their subsequent oxidation to nitrates.

In parallel with the "nitrite route," oxidation of NO to $NO_2$ on Pt sites by gaseous oxygen can also occur (route c); the $NO_2$ thus formed is stored on BaO directly in the form of nitrates ("nitrate route" = routes (c) + (d)), i.e., without the intermediacy of nitrites, according to a disproportionation reaction (route (d)). Despite the fact that NO release is involved in this route, a dead time in the $NO_x$ concentration could be observed due to oxidation of the released NO along the reactor axis [26]. Direct $NO_2$ uptake in the form of nitrate cannot be excluded, although it is of minor importance.

The "nitrite" and "nitrate" pathways operate simultaneously during $NO/O_2$ storage but the first, which is responsible for the formation of nitrites, dominates over the disproportionation route since nitrites are the most abundant species before $NO_x$ breakthrough. The role of the alumina support, which showed nonnegligible $NO_x$ adsorption capacity in the presence of $NO_2$, has not been considered in the scheme due to the almost complete coverage by the Ba component.

## 4. Conclusions

In this work, the transient response method, FT-IR spectroscopy, and TPD measurements were used as complementary techniques to gain information on the mechanisms of $NO_x$ storage on supported Pt–Ba catalysts and on the role of the different catalyst components. It was found that the most effective pathway for $NO_x$ storage from $NO/O_2$ mixtures is a "nitrite" route, which implies the stepwise oxidation of NO leading to the formation of nitrite ad-species. A cooperative interaction between Pt and a nearby Ba site is suggested for this route, which hence implies the existence of a Pt–Ba interaction on the $Al_2O_3$ support. Nitrites are then progressively oxidized into nitrate species, which are predominant at catalyst saturation.

In parallel with the formation of nitrite ad-species, oxidation of NO (on Pt sites) to $NO_2$ by gaseous oxygen can also occur; the $NO_2$ thus formed can be stored on BaO directly in the form of nitrates according to a disproportionation reaction which implies the release of one NO molecule for three molecules of $NO_2$ consumed ("nitrate" route). No nitrite formation has been observed in this route. As nitrites are the most abundant species before $NO_x$ breakthrough, it is concluded that the "nitrite" pathway dominates over the disproportionation route in the case of $NO/O_2$ adsorption over Pt–Ba/$\gamma$-$Al_2O_3$.

## Acknowledgment

This work was supported by MURST (Roma)—Cofin 2000: Project "Catalysis for the Reduction of the Environmental Impact of Mobile Sources."

## References

[1] M.R. Heck, J.R. Farrauto, Catalytic Air Pollution Control, Van Nostrand Reinhold, New York, 1995.
[2] S. Sato, Y. Yu-u, H. Yahiro, N. Mizuno, M. Iwamoto, Appl. Catal. 70 (1991) L1.
[3] M. Iwamoto, H. Hamada, Catal. Today 10 (1991) 51.
[4] R. Burch, P.I. Millington, A.P. Walker, Appl. Catal. B 4 (1994) 65.
[5] M. Shelef, Chem. Rev. 95 (1995) 209.
[6] N. Miyoshi, S. Matsumoto, K. Katoh, T. Tanaka, J. Harada, N. Takahashi, K. Yokota, M. Sugiura, K. Kasahara, SAE Technical Paper 950809, 1995.
[7] S. Matsumoto, Catal. Today 29 (1996) 43.
[8] N. Takahashi, H. Shinjoh, T. Iijima, T. Suzuki, K. Yamazaki, K. Yokota, H. Suzuki, N. Miyoshi, S. Matsumoto, T. Tanizawa, T. Tanaka, S. Tateishi, K. Kasahara, Catal. Today 27 (1996) 63.
[9] H. Shinjoh, N. Takahashi, K. Yokota, M. Sugiura, Appl. Catal. B 15 (1998) 189.
[10] L. Olsson, B. Westerberg, H. Persson, E. Fridell, M. Skoglundh, B. Andersson, J. Phys. Chem. B 1036 (1999) 104338.
[11] E. Fridell, H. Persson, B. Westerberg, L. Olsson, M. Skoglundh, Catal. Lett. 66 (2000) 71.
[12] P. Broqvist, I. Panas, E. Fridell, H. Persson, J. Phys. Chem. B 106 (2002) 137.
[13] N.V. Cant, M.J. Patterson, Catal. Today 73 (2002) 271.
[14] C. Hess, J.H. Lunsford, J. Phys. Chem. B 106 (2002) 6358.
[15] C. Hess, J.H. Lunsford, J. Phys. Chem. B 107 (2003) 1982.
[16] P.J. Schmitz, R.J. Baird, J. Phys. Chem. B 106 (2002) 4172.
[17] Ch. Sedlmair, K. Seshan, A. Jentys, J.A. Lercher, J. Catal. 214 (2003) 308.
[18] H.Y. Huang, R.Q. Long, R.T. Yang, Energy Fuels 15 (2001) 205.
[19] F. Prinetto, G. Ghiotti, I. Nova, L. Lietti, E. Tronconi, P. Forzatti, J. Phys. Chem. B 105 (2001) 12732.
[20] L. Lietti, P. Forzatti, I. Nova, E. Tronconi, J. Catal. 204 (2001) 175.
[21] G. Mestl, M.P. Rosynek, J.H. Lunsford, J. Phys. Chem. B 102 (1998) 154.
[22] I. Nova, L. Castoldi, L. Lietti, E. Tronconi, P. Forzatti, Catal. Today 75 (2002) 431.
[23] L. Castoldi, I. Nova, L. Lietti, E. Tronconi, P. Forzatti, Chem. Eng. Trans. 3 (2003) 117.
[24] F. Prinetto, G. Ghiotti, I. Nova, L. Castoldi, L. Lietti, P. Forzatti, Phys. Chem. Chem. Phys. 5 (2003) 4428.
[25] I. Nova, L. Castoldi, F. Prinetto, V. Dal Santo, L. Lietti, E. Tronconi, P. Forzatti, G. Ghiotti, R. Psaro, S. Recchia, Top. Catal., in press.
[26] A. Scotti, I. Nova, E. Tronconi, L. Castoldi, L. Lietti, P. Forzatti, IECR, submitted for publication.
[27] L. Olsson, E. Fridell, J. Catal. 210 (2002) 340.
[28] G. Fornasari, F. Trifirò, A. Vaccari, F. Prinetto, G. Ghiotti, G. Centi, Catal. Today 75 (2002) 421.